

N12-28171

NASA TECHNICAL  
MEMORANDUM



NASA TM X-2606

NASA TM X-2606

CASE FILE  
COPY

HALL CURRENT EFFECTS IN THE LEWIS  
MAGNETOHYDRODYNAMIC GENERATOR

by Lester D. Nichols and Ronald J. Sovie

Lewis Research Center  
Cleveland, Ohio 44135

NATIONAL AERONAUTICS AND SPACE ADMINISTRATION • WASHINGTON, D. C. • JULY 1972

1. Report No. <b>NASA TM X-2606</b>	2. Government Accession No.	3. Recipient's Catalog No.	
4. Title and Subtitle <b>HALL CURRENT EFFECTS IN THE LEWIS MAGNETOHYDRODYNAMIC GENERATOR</b>		5. Report Date <b>July 1972</b>	6. Performing Organization Code
7. Author(s) <b>Lester D. Nichols and Ronald J. Sovie</b>		8. Performing Organization Report No. <b>E-6924</b>	10. Work Unit No. <b>112-02</b>
9. Performing Organization Name and Address <b>Lewis Research Center National Aeronautics and Space Administration Cleveland, Ohio 44135</b>		11. Contract or Grant No.	13. Type of Report and Period Covered <b>Technical Memorandum</b>
12. Sponsoring Agency Name and Address <b>National Aeronautics and Space Administration Washington, D.C. 20546</b>		14. Sponsoring Agency Code	
15. Supplementary Notes			
16. Abstract <p>Data obtained in the Lewis MHD generator are compared with theoretical values calculated by using the Dzung theory. The generator is operated with cesium seeded argon as the working fluid. The gas temperature varies from 1800 to 2100 K, the gas pressure from 19 to 22 N/cm<sup>2</sup>, the Mach number from 0.3 to 0.5, and the magnetic field strength from 0.2 to 1.6 T. The analysis indicates that there is incomplete seed vaporization and that Hall current shorting paths (through the working fluid to ground at both the entrance and exit of the channel) limit generator performance.</p>			
17. Key Words (Suggested by Author(s)) <b>Magnetohydrodynamic generator Hall current</b>		18. Distribution Statement <b>Unclassified - unlimited</b>	
19. Security Classif. (of this report) <b>Unclassified</b>	20. Security Classif. (of this page) <b>Unclassified</b>	21. No. of Pages <b>26</b>	22. Price* <b>\$3.00</b>

\* For sale by the National Technical Information Service, Springfield, Virginia 22151

# HALL CURRENT EFFECTS IN THE LEWIS MAGNETOHYDRODYNAMIC GENERATOR

by Lester D. Nichols and Ronald J. Sovie

Lewis Research Center

## SUMMARY

Data obtained in the Lewis magnetohydrodynamic (MHD) Faraday segmented generator are analyzed by using theoretically computed values of the conductivity and mobility and the finite segmentation theory of Dzung, which includes axial current leakage. The generator is operated with cesium seeded argon as the working fluid. The gas temperature varies from 1800 to 2100 K, the gas pressure from 19 to 22 newtons per square centimeter, the Mach number from 0.3 to 0.5, and the magnetic field strength from 0.2 to 1.6 teslas.

Analysis of results is based on the fact that the electrical characteristics of an MHD generator depend upon the loading resistances in the Hall and Faraday directions, the working fluid state, and the magnetic field strength. If the generator is shorted in the Faraday direction for known magnetic field strength and argon conditions, the two remaining unknowns are the cesium seed fraction and Hall load resistance. The Faraday current and Hall voltage are sensitive to these unknowns, and their values are used to determine the unknown seed fraction and Hall load resistance by using the Dzung calculation. The results show that the seed concentration depends strongly upon the spray bar orientation and duct geometry and that the Hall load resistance is proportional to the plasma resistivity.

The calculation of the Faraday resistance could also be made by using the Dzung model. The result indicates high resistance in the Faraday direction that is comparable to the value measured without cesium in the duct. This implies that the plasma shorts the generator in the Hall direction but not in the Faraday direction.

As a result of these analyses, it is concluded that there is incomplete seed vaporization and a shorting path for the generated Hall current through the plasma itself to ground at both the entrance and exit of the channel.

## INTRODUCTION

The NASA Lewis closed-loop magnetohydrodynamic (MHD) generator was designed to study power generation with nonequilibrium ionization by using a cesium seeded argon plasma. The primary experimental program is to evaluate the feasibility of generating MHD power for space with input gas temperatures of 2000 to 2100 K through the use of nonequilibrium ionization. The success of this program could lead to lower weight space power generation systems as well as higher efficiency ground-based power generation systems (ref. 1). In the latter case, the increased efficiency could result in a significant reduction in air and thermal pollution.

The theoretical performance of the Lewis (Brayton cycle) MHD generator was evaluated by Heighway and Nichols (ref. 2). In a power generation experiment, however, there are many parameters that can cause the performance to be different from the ideal values predicted by theory. The open-circuit voltage can be affected by current shorting paths either through the insulator walls or through the gas (ref. 3). The short-circuit current can be affected by the same shorting paths, by electrode voltage drops, and by plasma conditions. The plasma conditions include conductivity and uniformity. If the Hall parameter is large enough, nonuniformities can significantly affect performance, especially for segmented generators (Rosa, ref. 4).

In this report several nonideal effects are examined and the calculated generator performance is compared with experimental measurements in the Lewis MHD generator.

## OPERATING CONDITIONS

### Generator Geometry

The Lewis MHD generator facility has been described elsewhere (refs. 5 and 6). For purposes of comparison with theories, the geometry must be specified and is shown in figure 1(a). The generator is 6.3 centimeters between the insulating walls and 20 centimeters between the conductor walls. There are 28 segmented electrodes which are 1.3 centimeters wide and are separated by insulators 1.3 centimeters wide. One set of data was taken with a generator which was 3.8 centimeters between the insulating side walls.

### Working Fluid Conditions

Tests were run over a wide range of operating conditions. In all cases the working fluid was argon seeded with cesium. The total temperature and pressure for the various

runs are given in table I. The entrance Mach number is also given in table I. The Mach number changes only slightly along the channel. The actual cesium seed fraction is considered as an unknown. The rate at which the liquid cesium leaves the supply pot and enters the vaporizer is monitored for each run. From that mass flow rate and the gas flow rate an average seed fraction is determined. However, since the quality of the vapor leaving the vaporizer is not accurately known, and since there are indications that cesium is still present even after the seed valve is closed, the cesium vapor seed rate is considered as an unknown. Tests were made with the cesium vapor injection bar oriented in the upstream and downstream directions, as indicated in table I. Furthermore, in run 6, mixing bars were added downstream of the vaporizer to promote better seed mixing.

The magnetic field strengths for runs 1 to 6 were varied from 0.1 to 1.6 teslas. The Mach number was varied from 0.3 to 0.5.

### Load Conditions

The current carrying paths are difficult to characterize. The leakage current flows through paths whose resistance may change when cesium is present, if the leakage current is carried by the plasma. We will assume that the resistances of the various current carrying paths are not known.

### NONIDEAL EFFECTS

#### Fluctuations

The current (even under short-circuit conditions) is less than 0.1 ampere per square centimeter. There are impurities of carbon monoxide and hydrogen in the loop. The minimum concentration is 1000 ppm of each. For these conditions, the electron temperature will not be much greater than the gas temperature, so the ionization instabilities are not present (ref. 7). As a result, we will assume that the effective values of conductivity and Hall parameter are equal to the calculated values. As the current density increases, we will have to include instabilities in our analysis.

#### Electrode Voltage Drops

We have measured the potential profile for the generator and have found no cathode voltage drops. This is in agreement with the conclusion that there is sufficient ther-

mionic emission from the cathodes for the calculated values of seed concentration and the cathode temperature. At higher currents achieved when voltages are applied to the cathodes there is a sheath voltage that is required.

## Finite Segmentation

The Hall parameters can get rather large (of the order of 10) so that segmentation effects can be considerable, especially for the Hall voltage. We will consider this effect in our analysis.

## Nonuniformities

The walls of the channel are nearly the same temperature as the gas, so there will be a small thermal boundary layer. The velocity boundary layer is too small to affect significantly the results of the measurements in channels the size of the Lewis channel. As a result, we will use the velocity determined from the mass flow rate and uniform density.

## Mathematical Model of Generator Current and Voltage

The mathematical model used is merely an extension of the results of Dzung (ref. 3). He assumes uniform plasma properties and velocity profiles. As a result of his analysis, it is possible to account for electrode segmentation effects and current leakages in the Faraday and Hall directions. Dzung's analysis considers the results for a single pair of electrodes out of a number of electrodes. That is, he considers each  $i^{th}$  electrode pair as an independent generator with Faraday and Hall voltages  $V_y$  and  $V_x$  and load resistances  $R_y$  and  $R'_x$ , respectively. The voltages in the Faraday and Hall directions are given by (see fig. 1(b) for sketch):

$$V_y = \frac{\alpha h UB}{\alpha + 2\rho u + (1 + 2\rho v)\tan \theta} \quad (1)$$

$$V_x = \frac{l UB}{\alpha + 2\rho u + (1 + 2\rho v)\tan \theta} \quad (2)$$

and the currents by

$$I_y = \frac{V_y}{R_y} \quad (3)$$

$$I_x = \frac{V_x}{R'_x} \quad (4)$$

where the  $R$ 's are the effective resistances that each generator "sees" and include all internal leakage resistances. (Symbols are defined in appendix A.)

In our analysis we wish to extend these results to predict the overall performance of a generator with  $N$  electrode pairs. In the Faraday direction the results are unchanged since the  $R_y$ 's for each electrode pair are uncoupled. The results are more complicated in the Hall direction, however, since each of the  $i$  generators is connected in series and one must consider two leakage paths. There is the leakage resistance for each  $i^{\text{th}}$  electrode pair  $R_{x,i}$  and the leakage of the generator as a whole  $R_{x,o}$ . The equivalent circuit for determining the Hall voltage is shown in appendix B. It is shown in appendix B that the Dzung equations can be used to predict the overall generator performance if the  $R'_x$  in equation (4) is replaced by

$$R'_x = \frac{R_{x,i} R_{x,o}}{N R_{x,i} + R_{x,o}} \quad (5)$$

It is convenient to consider the resistance for  $N$  such generators, so

$$R_x = N R'_x$$

will be introduced. Then,

$$R_x = \frac{N R_{x,i} R_{x,o}}{N R_{x,i} + R_{x,o}}$$

It can be seen that, if  $N R_{x,i} \gg R_{x,o}$ ,

$$R_x = R_{x,o}$$

Then the quantities  $\theta'$ ,  $K$ ,  $2\rho$ , and  $\alpha$  in equations (1) and (2) are given by

$$\theta' = 90^\circ + \tan^{-1} \left( \frac{\beta K + 2\rho u}{1 + K + 2\rho v} \right) - \tan^{-1} \beta \quad (6)$$

$$K = \frac{l}{R'_x h W \sigma} \quad (7)$$

$$2\rho = \frac{l}{h} \quad (8)$$

$$\alpha = \frac{l \sigma W R_y (1 + 2\rho v + K)}{h [(1 + 2\rho v)\beta - 2\rho u]} \quad (9)$$

The terms  $u$  and  $v$  are functions of the Hall parameter and the ratio of electrode width to insulator width. These functions have been calculated by Dzung and are plotted in reference 3. The Lewis MHD generator is built with electrode width equal to insulator width. The functions  $u$  and  $v$  for this case ( $c = 1/2$  in Dzung's notation) can be approximated by the quadratic functions

$$u = 1.109 \times 10^{-4} + 6.829 \times 10^{-3} (\tan^{-1} \beta) - 1.371 \times 10^{-5} (\tan^{-1} \beta)^2 \quad (10)$$

$$v = 2.208 \times 10^{-1} - 1.769 \times 10^{-4} (\tan^{-1} \beta) - 2.564 \times 10^{-5} (\tan^{-1} \beta)^2 \quad (11)$$

where  $\tan^{-1} \beta$  is given in degrees. Using these equations, one can predict the voltages and currents in the generator by specifying the loading resistances  $R_y$  and  $R_x$ , the working fluid state ( $\sigma$ ,  $\mu_e$ , and  $U$ ), the generator geometry, and the magnetic field strength  $B$ .

## METHOD OF DATA ANALYSIS

### Determination of Seed Fraction and Hall Resistance

In the generator tests, the working fluid state is completely determined except for the cesium seed fraction. As was stated in the section Working Fluid Conditions, the average liquid cesium flow rate into the vaporizer and spray bar is measured. However, the quality of the vapor leaving the spray bar is not known; therefore, the vapor seed rate is considered as an unknown.

The generator is run short circuited in the Faraday direction ( $R_y = 0$ ) with an external open circuit in the Hall direction. The measured value of the Hall voltage is then an indication of the internal Hall resistance. Thus, with the working fluid state, magnetic field strength, and externally applied loads specified, the only unknown parameters are the cesium seed fraction and internal Hall leakage resistance. For a given pair of values for the seed fraction and Hall resistance, equations (1) to (9) can be used to calculate a value of the Hall voltage and Faraday short-circuit current. Note that  $I_y$  can be determined from equation (3) at  $R_y = 0$  since  $V_y$  is proportional to  $R_y$ . Then two families of curves can be generated, one keeping the resistance constant and varying the seed fraction, and the other keeping the seed fraction constant and varying the resistance. These curves then give the complete performance characteristic of  $I_y$  as a function of  $V_x$  for the run conditions specified and a given magnetic field. The position of the measured Faraday current and measured Hall voltage on this characteristic plot then yields the value of seed fraction and Hall resistance present in the generator. Such a performance characteristic for experimental run 6 is shown in figure 2 for  $B = 0.5$  T. The measured data at this magnetic field are indicated by the circle.

Using this method then, it is possible to obtain values for the seed fraction and Hall resistance that fit the data for each magnetic field strength tested. The seed fraction and Hall resistance obtained for run 6 are plotted against magnetic field strength in figure 3. The points at low magnetic field strength (0.15 and 0.25 T) were taken immediately after the cesium valve was opened. Apart from these two points which are affected by transient effects in the vaporizer, it appears that the seed fraction was constant at about  $8 \times 10^{-4}$ . Similarly, the Hall resistance is about 5 ohms. Curves of the calculated values of  $I_y$  and  $V_x$  as a function of  $B$  for these values of  $s$  and  $R_x$  are shown in figure 4. The measured data points are also shown in this figure.

### Determination of Faraday Resistance

The values of seed concentration and Hall resistance can be determined as described previously by running tests with  $R_y$  shorted out. If, however, during one of these tests the load circuit switch is opened, the Faraday open-circuit voltage is measured. Using this open-circuit voltage and the seed fraction and Hall resistance obtained before opening the switch, one can determine  $R_y$ .

### Applied Voltage Tests

Because of the low values of  $R_x$  obtained in the generator, the generated Hall voltage is quite low, and this in turn limits the values of the generated Faraday current.

In an attempt to increase the value of the Faraday current and obtain results at higher Hall voltage, an external power supply was used to simulate the Hall voltage. The power supply was hooked from electrode pair 6 to 17, so for this case the length of the generator is 28 centimeters and the number of electrodes N is 11. It is shown in appendix C that, if you neglect the possibility that fluctuations can develop at the increased current densities, Dzung's analysis can be extended to predict the current increase as a function of Hall voltage.

## RESULTS AND DISCUSSION

### Seed Fraction

A comparison of the results obtained for the various operating conditions and channel configurations given in table I is shown in table II for a magnetic field of about 1 tesla. The calculations of the seed fraction presented in figure 3 indicated that after some initial transient effects the seed fraction reached a fairly steady value. This steady value is less than the value determined from the liquid flow rate out of the cesium container, as is shown in table II. The low value for the seed fraction is due to incomplete vaporization. Comparison of the seed fraction actually obtained with the liquid injection rate for the different runs confirms this. The fraction of seed vaporized with the vaporizer injection tube oriented in the upstream direction (runs 2 and 5) is about 10 percent, whereas it is only a few percent for the downstream orientation. Furthermore, the addition of the mixing bars increased the fraction vaporized to 30 percent.

### Hall Resistance

The values of the Hall resistance  $R_x$  obtained are quite small compared to measurements made prior to the cesium injection. In order to arrive at an explanation of this, the plasma resistivity is plotted as a function of the Hall resistance in figure 5 for all the various run conditions listed in table II. The figure shows that there is a correlation between the two indicating that a significant portion of the  $R_x$  value is through the plasma itself. If one assumes that the total resistive path is in the duct, the length of this path L can be determined from the relation  $L = hWR_x/r$ . Using the value  $r = 0.67$  ohm-meter when  $R_x = 100$  ohms from figure 6, one calculates the  $L = (1/0.67)(0.20)(0.0635)(100) = 1.9$  meters.

It is seen from figure 1 that this length is comparable to the distance from the vaporizer spray bar to the generator entrance plus the distance from the generator exit to the re heater. The re heater is grounded, and despite efforts to float the spray bar, a

voltmeter monitoring the voltage to ground indicates that it often becomes grounded during the cesium injection.

## Faraday Resistance

The Faraday load resistance  $R_y$  was obtained in one run for the operating conditions of run 6 and a variable magnetic field strength. The data analysis indicated  $R_x = 6$  ohms,  $R_y = 300$  ohms, and  $s = 6.6 \times 10^{-4}$ . The variation of  $V_y$ ,  $V_x$ , and  $I_y$  with magnetic field strength that is predicted by the analysis for these values of  $R_x$ ,  $R_y$ , and  $s$  is represented by the curves in figure 6. The measured data points are also shown in this figure. The figure shows that there is good agreement between the analysis and measured results. The large  $R_y$  value obtained eliminates the possibility that the low  $R_x$  values are caused by the electrodes being shorted to the stainless steel case since this would also cause  $R_y$  to be low.

## Applied Hall Voltage Tests

As was previously mentioned, a test was run with a power supply connected from electrode pair 6 to 17 in order to increase the Hall voltage and Faraday current. This test was performed for the gas conditions of run 6 and a magnetic field strength of 0.47 tesla. The variation of the Faraday current with Hall voltage is shown in figure 7. The power supply voltage  $V_a$  is also indicated in the figure. The power supply resistance  $R_a$  was 10 ohms. The solid lines in the figure are those predicted by the analysis in appendix C for  $R_y = 0$ ,  $R_x = 11$  ohms, and  $s = 0.002$  to  $0.00025$ . The measured data are indicated by the data points. The figure shows that the Faraday current does indeed increase with increasing Hall voltage and that the analysis adequately predicts this behavior.

The  $R_x$  value of 11 ohms can be compared with the 10 ohm value obtained for the whole generator ( $N = 28$ ) before the power supply was used. These values can be used to show that the main shorting loop is external to the generator (i. e., that  $NR_{x,i} > R_{x,o}$ ). The value of  $R_{x,o}$  is assumed to depend on the length of plasma from the vaporizer to the generator entrance plus the length from the generator exit to the re-heater. This length changes from about 190 centimeters (based on fig. 7) for  $N = 28$  to 234 centimeters for  $N = 11$ . Using equation (B9), then, to evaluate  $R_x$  without the power supply, we have

$$\frac{1}{R_x} = \frac{1}{28R_{x,i}} + \frac{1}{R_{x,o}} = \frac{1}{10}$$

and with the power supply

$$\frac{1}{R_x} = \frac{1}{11R_{x,i}} + \frac{190}{(R_{x,o})(234)} = \frac{1}{11}$$

The solution to these two equations is  $R_{x,o} = 10.6$  ohms and  $R_{x,i} = 6.3$  ohms. Thus, the internal resistance  $NR_{x,i}$  is large compared to the external resistance.

### Generated Power

The amount of power generated can be increased by increasing the applied voltage. The difference between power generated and power applied is plotted in figure 8 as a function of  $R_x$  (for  $N = 11$ ). The applied voltage  $V_a$  is a parameter. It can be seen that the amount of power required is always greater than that generated. At large enough values of  $R_x$  the power applied approaches zero.

### Cathode Voltage Drops

The amount of current that is flowing in the generator can be supplied by thermionic emission from a tungsten electrode in a partial pressure cesium atmosphere. From the Langmuir results (ref. 8) the maximum thermionic emission current for each case can be calculated for the assumed seed concentration. This maximum  $j_{e,max}$  is shown in table I. In all cases (except for run 4) one would expect no sheath voltage at the cathode.

### CONCLUDING REMARKS

The good agreement between the behavior predicted by the extension of Dzung's analysis and the data indicates that this analysis can be a useful tool for understanding generator performance. As a result of using the analysis to reduce the data obtained in NASA Lewis MHD generator experiments, the following problem areas were indicated. There is incomplete seed vaporization, and there is an axial shorting loop from the cesium injection bar through the plasma to the grounded reheater. These problems are presently being remedied.

It was also found that applying a voltage in the Hall direction does improve the power generation from the generator. The amount of power required increases with decreasing

leakage resistance. This technique may prove useful if the Hall resistance can be increased.

Lewis Research Center,  
National Aeronautics and Space Administration,  
Cleveland, Ohio, May 8, 1972,  
112-02.

## APPENDIX A

### SYMBOLS

$A_e$	electrode area
$B$	magnetic field strength
$E$	electric field
$h$	distance between electrodes
$I$	current
$j$	current density
$K$	resistance ratio in Hall direction
$L$	generator length
$l$	distance between adjacent electrodes
$N$	number of electrodes
$P$	power
$R$	resistance
$r$	resistivity
$U$	gas velocity
$u, v$	parameters defined by Dzung
$V$	generator voltage
$W$	channel width
$\alpha$	Faraday load voltage load factor
$\beta$	Hall parameter
$\epsilon$	current angle
$\theta'$	angle between flow direction and electric field
$\mu_e$	electron mobility
$\rho$	ratio of electrode width to distance between electrodes
$\sigma$	conductivity
$\tau$	Hall angle

Subscripts:

a applied

i electrode number

o overall generator

x Hall

y Faraday

## APPENDIX B

### EXTENSION OF DZUNG'S RESULTS TO PREDICT OVERALL GENERATOR PERFORMANCE

The analysis of Dzung was made for a single pair of electrodes out of a number of electrodes. The situation is equivalent to the  $i^{\text{th}}$  generator shown in figure 9. The results for the  $i^{\text{th}}$  generator can be used to calculate the results for an  $N$ -electrode pair generator by using the schematic diagram shown in figure 9.

The voltages in the  $i^{\text{th}}$  generator are

$$V_i = I_i R_i + I_{x,i} R_{x,i} \quad (\text{B1})$$

The current flowing through  $R_{x,i}$  is

$$I_{x,i} = I_i - I_{x,o} \quad (\text{B2})$$

This can be proved by mathematical induction. It is certainly true that  $I_{x,1} = I_1 - I_{x,o}$ . If one assumes that  $I_{x,i} = I_i - I_{x,o}$  and uses the fact that

$$I_{x,i+1} + I_i = I_{i+1} + I_{x,i}$$

then one derives

$$I_{x,i+1} = I_{i+1} - I_{x,o}$$

Substituting equation (B2) into (B1), we have

$$V_i = I_i(R_i + R_{x,i}) - I_{x,o}R_{x,i} \quad (\text{B3})$$

Considering the voltage drop  $V_{x,o}$  across  $R_{x,o}$ , which is given by

$$V_{x,o} = I_{x,o}R_{x,o} = \sum_{i=1}^N I_{x,i}R_{x,i} = \sum_{i=1}^N (V_i - I_i R_i) \quad (\text{B4})$$

and solving equation (B3) for  $I_i$  yield

$$I_i = \frac{V_i + V_x \frac{R_{x,i}}{R_{x,o}}}{R_{x,i} + R_i} \quad (B5)$$

If  $V_{x,i} = I_{x,i} R_{x,i}$ , using equations (B1) and (B5) results in

$$V_{x,i} = V_i \frac{R_{x,i}}{R_{x,i} + R_i} - V_{x,o} \frac{R_{x,i} R_i}{R_{x,o}(R_{x,i} + R_i)} \quad (B6)$$

Summation of equation (B6) over the  $i$  generators and solving for  $V_{x,o}$  yield

$$V_{x,o} = \frac{\sum_{i=1}^N \frac{V_i R_{x,i}}{R_i + R_{x,i}}}{1 + \frac{1}{R_{x,o}} \sum_{i=1}^N \frac{R_i R_{x,i}}{R_{x,i} + R_i}} \quad (B7)$$

Substitute  $V_{x,o}$  from equation (B7) into equation (B6) and solve for  $V_{x,i}$ .

$$V_{x,i} = \frac{V_i R_{x,i}}{R_{x,i} + R_i} - \frac{R_{x,i} R_i}{R_{x,o}(R_{x,i} + R_i)} \frac{\sum_{i=1}^N \frac{V_i R_{x,i}}{R_i + R_{x,i}}}{1 + \frac{1}{R_{x,o}} \sum_{i=1}^N \frac{R_i R_{x,i}}{R_{x,i} + R_i}} \quad (B8)$$

Then, if all of the generators are the same,

$$\frac{V_{x,i}}{V_i} = \frac{\frac{R_{x,i} R_{x,o}}{R_{x,o} + N R_{x,i}}}{\frac{R_{x,i} R_{x,o}}{R_{x,o} + N R_{x,i}} + R_i} = \frac{V_x}{N V_i}$$

Therefore, the voltage of the total generator is just  $N$  times the voltage of each generator, and the voltage of each generator can be determined from the open-circuit voltage  $V_i$  and the internal impedance  $R_i$  by assuming that the load resistance is

$$R'_x = \frac{R_{x,i}}{1 + \frac{N R_{x,i}}{R_{x,o}}}$$

This is merely the parallel combination of  $R_{x,i}$  and  $R_{x,o}/N$ . If one defines an overall leakage resistance for the Hall direction as  $R_x'$ , then

$$\frac{1}{R_x'} = \frac{1}{N R_{x,i}} + \frac{1}{R_{x,o}} \quad (B9)$$

where

$$N R_x' \equiv R_x$$

## APPENDIX C

### EXTENSION OF DZUNG ANALYSIS TO INCLUDE APPLIED POWER SUPPLY

The schematic diagram for the MHD generator with an applied voltage in the Hall direction over some of the electrodes is shown in figure 10. The relation between current and voltage for the circuit is

$$\left( \frac{1}{R_a} + \frac{1}{NR_{x,i}} + \frac{1}{R_{x,o}} \right) V_x + \frac{1}{R_{x,o}} V_{x,i} = \frac{V_a}{R_a} + I_x \quad (C1)$$

If  $V_{x,i} \ll V_x$ , and

$$\frac{1}{R_x} \equiv \frac{1}{NR_{x,i}} + \frac{1}{R_{x,o}}$$

then equation (C1) can be written as

$$V_x = \frac{R_x R_a}{R_x + R_a} I_x + \frac{R_x}{R_a + R_x} V_a \quad (C2)$$

The values of  $V_x$  and  $I_x$  are given by Dzung (ref. 3) as

$$V_x = \frac{LUB \cos \theta'}{(\alpha + 2\rho u) \cos \theta' + (1 + 2\rho v) \sin \theta'} \quad (C3)$$

$$I_x = \frac{\sigma h W U B \cos \tau \cos \epsilon [(1 + 2\rho v) \tan \epsilon - 2\rho u]}{(\alpha + 2\rho u) \cos \theta' + (1 + 2\rho v) \sin \theta'} \quad (C4)$$

The angle of the current vector  $\epsilon$  can be found by substituting equations (C4) and (C3) into (C2) by using  $\theta' = \pi/2 - \tau + \epsilon$  and solving for  $\tan \epsilon$ :

$$\tan \epsilon = \frac{B + \frac{R_x R_a}{R_x + R_a} \frac{2\rho u \sigma h W}{L} - \frac{R_x}{R_x + R_a} \frac{V_a}{LUB} [1 + \sigma W R_y + 2\rho(v + u\beta)]}{1 + (1 + 2\rho v) \left( \frac{R_x R_a}{R_x + R_a} \frac{\sigma h W}{L} + \frac{\beta R_x}{R_a + R_x} \cdot \frac{V_a}{LUB} \right) - 2\rho u \frac{R_x}{R_x + R_a} \frac{V_a}{LUB}} \quad (C5)$$

The value of  $\epsilon$  can now be used in the analysis of the current and voltage.

## REFERENCES

1. Seikel, G. R.; and Nichols, L. D.: The Potential of Nuclear MHD Electric Power Systems. Paper 71-638, AIAA, June 1971.
2. Heighway, John E.; and Nichols, Lester D.: Brayton Cycle Magnetohydrodynamic Power Generation with Nonequilibrium Conductivity. NASA TN D-2651, 1965.
3. Dzung, L. S.: Influence of Wall Conductance on the Performance of MHD Generators with Segmented Electrodes. Electricity from MHD vol. II IAEA, Vienna, 1966, pp. 169-176.
4. Rosa, R. J.: Hall and Ion-Slip Effects in a Nonuniform Gas. Phys. Fluids, vol. 5, no. 9, Sept. 1962, pp. 1081-1090.
5. Nichols, Lester D.; Morgan, James L.; Nagy, Lawrence A.; Lamberti, Joseph M.; and Ellson, Robert A.: Design and Preliminary Operation of the Lewis Magnetohydrodynamic Generator Facility. NASA TN D-4867, 1968.
6. Sovie, R. J.; and Nichols, L. D.: Status of Power Generation Experiments in the NASA Lewis Closed-Cycle MHD Facility. Paper 72-103, AIAA, Jan. 1972.
7. Bishop, Allan R.; and Nichols, Lester D.: Conductivity of an Impure, Nonequilibrium Plasma with Electrothermal Instabilities. AIAA J., vol. 8, no. 4, Apr. 1970, pp. 829-831.
8. Langmuir, Irving: Phenomena, Atoms and Molecules. Philosophical Library, 1949, p. 341.

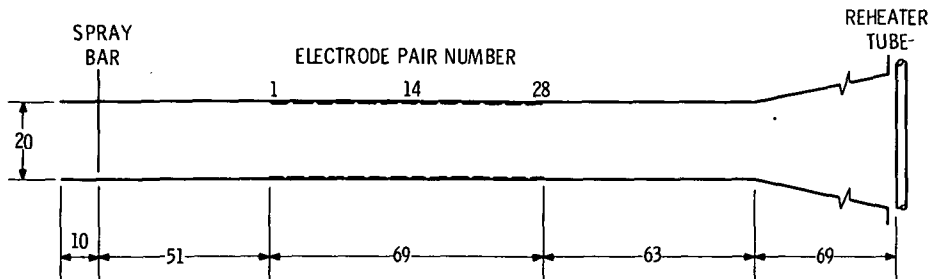
TABLE I. - EXPERIMENTAL OPERATING CONDITIONS AND CHANNEL CONFIGURATIONS

Operating condition	Run					
	1	2	3	4	5	6
Total gas temperature, K	1960	1950	1950	1897	1895	2091
Total gas pressure, N/cm <sup>2</sup>	22	21	21	21	19	21
Gas velocity, m/sec	424	336	313	316	323	264
Mach number	0.54	0.42	0.39	0.40	0.41	0.32
Channel height, cm	20	20	20	20	20	20
Channel width, cm	3.8	6.3	6.3	6.3	6.3	6.3
Vaporizer orientation	Upstream	Upstream	Downstream	Downstream	Upstream	Upstream
Mixing bars	No	No	No	No	No	Yes

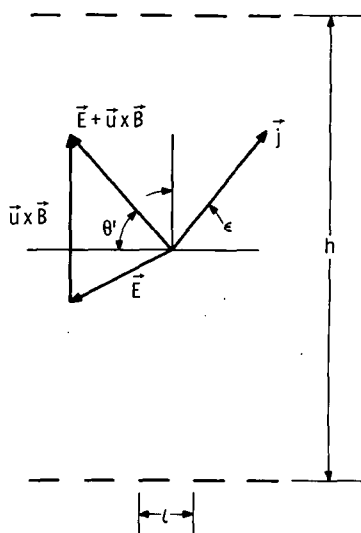
TABLE II. - EXPERIMENTAL RESULTS FOR MAGNETIC FIELD STRENGTH

## OF APPROXIMATELY 1 TESLA

Operating condition	Run					
	1	2	3	4	5	6
Total gas temperature, K	1960	1950	1950	1897	1895	2091
Magnetic field strength, T	0.9	1.0	1.0	1.0	0.96	1.07
Short-circuit current, A	0.079	0.050	0.065	0.011	0.085	0.370
Hall voltage, V	49	27	45	20	72	40
Liquid seed fraction	$29 \times 10^{-4}$	$23 \times 10^{-4}$	$63 \times 10^{-4}$	$34 \times 10^{-4}$	$44 \times 10^{-4}$	$30 \times 10^{-4}$
Calculated seed fraction	$11.5 \times 10^{-4}$	$2.8 \times 10^{-4}$	$2.1 \times 10^{-4}$	$0.16 \times 10^{-4}$	$4.3 \times 10^{-4}$	$9.0 \times 10^{-4}$
Fraction of seed vaporized	0.40	0.12	0.03	0.006	0.098	0.30
Conductivity, mho/m	5.0	5.8	5.7	1.3	4.9	20.4
Electron mobility, m <sup>2</sup> /Wb	7.8	12.3	12.7	15.3	12.1	7.6
Hall load resistance, R <sub>x</sub> , Ω	25	14	26.5	122	48	4.8
Current density, mA/cm <sup>2</sup>	4.9	3.1	4.0	0.68	5.3	22.9
Emission current density, mA/cm <sup>2</sup>	540	10	5	0.4	90	150



(a) DUCT, DIFFUSER, AND REHEATER TUBE LOCATION. DUCT WIDTH, 6.3 CENTIMETERS. (DIMENSIONS GIVEN IN CENTIMETERS.)



(b) CURRENT DENSITY AND ELECTRIC FIELD VECTOR ORIENTATION.

Figure 1. - Sketches showing geometry of MHD generator facility.

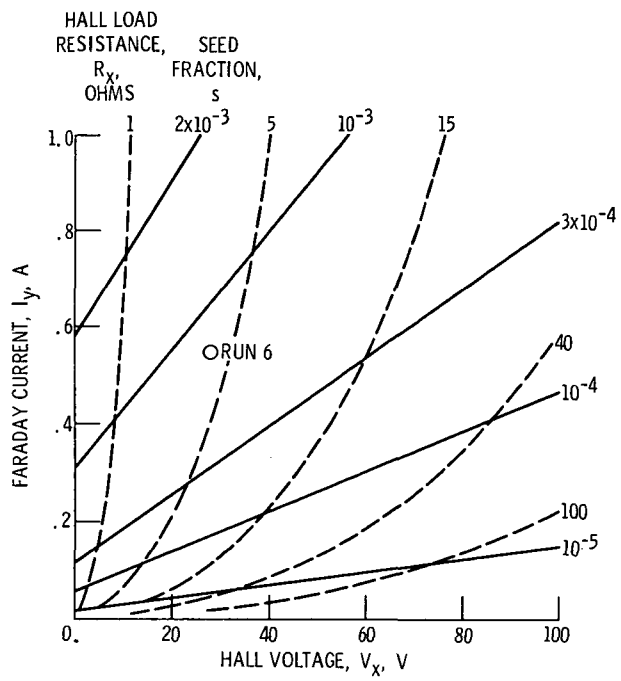


Figure 2. - Characteristics of Lewis MHD generator. Gas temperature, 2091 K; gas pressure, 21 newtons per square centimeter; gas velocity, 270 meters per second; magnetic field strength, 0.5 tesla.

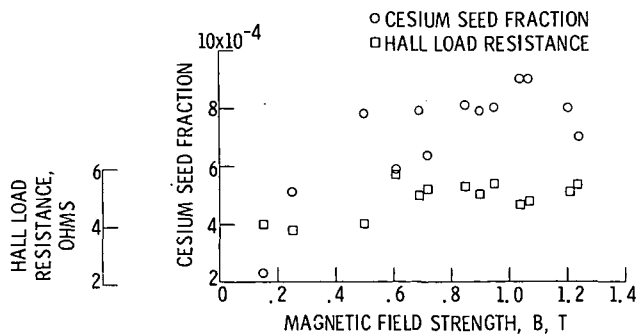


Figure 3. - Seed fraction and Hall leakage resistance as function of magnetic field strength for run 6.

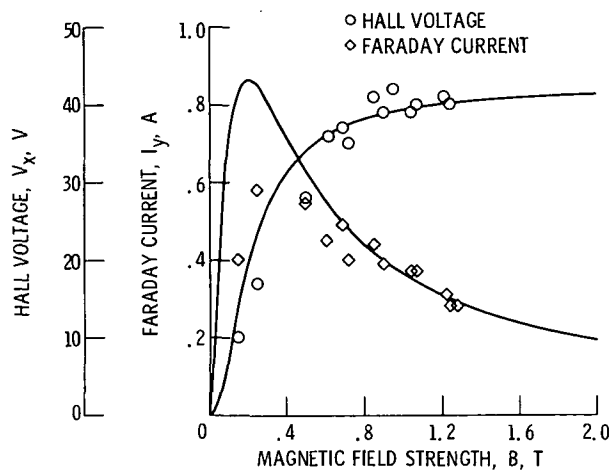


Figure 4. - Comparison of experimental data with calculated values.  
Gas temperature, 2091 K; gas pressure, 21 newtons per square centimeter; gas velocity, 270 meters per second.

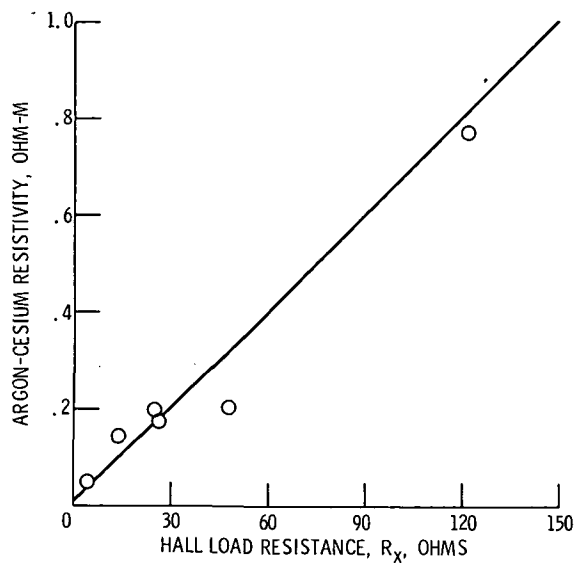


Figure 5. - Correlation between Hall load resistance and plasma resistivity for six runs.

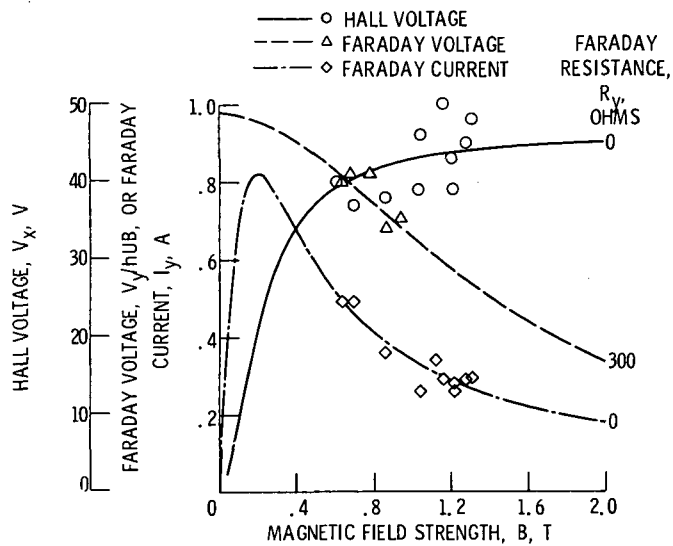


Figure 6. - Comparison of experimental data with calculated values.  
Gas temperature, 2091 K; gas pressure, 21 newtons per square centimeter; gas velocity, 270 meters per second.

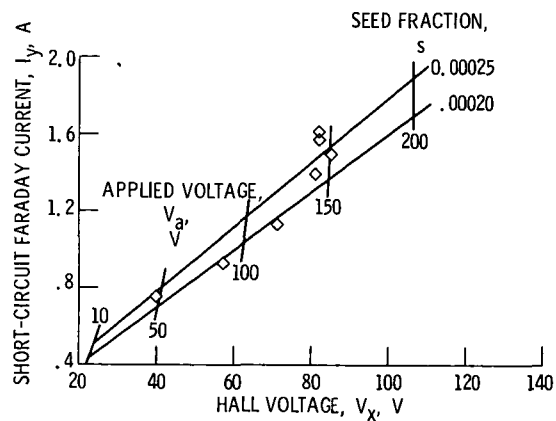


Figure 7. - Comparison of calculated current with measured current with applied power supply. Temperature, 2091 K; gas pressure, 21 newtons per square centimeter; Mach number, 0.316; generator length, 28 centimeters; magnetic field strength, 0.47 tesla; applied resistance, 10 ohms; Hall resistance, 11 ohms; Faraday resistance, zero.

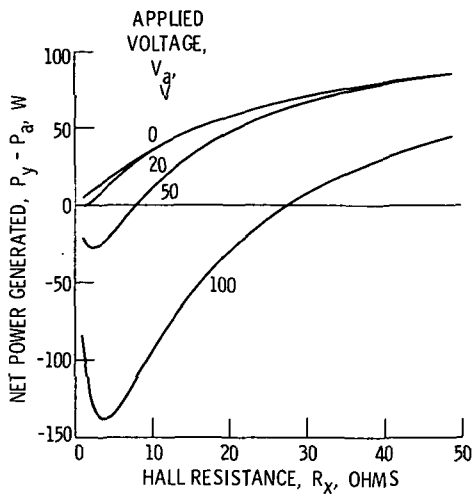


Figure 8. - Net generated power as function of Hall resistance. Temperature, 2091 K; gas pressure, 21 newtons per square centimeter; Mach number, 0.32; supply resistance, 10 ohms; Faraday resistance, 30 ohms; seed fraction,  $6.6 \times 10^{-4}$ ; number of electrode pairs, 11.

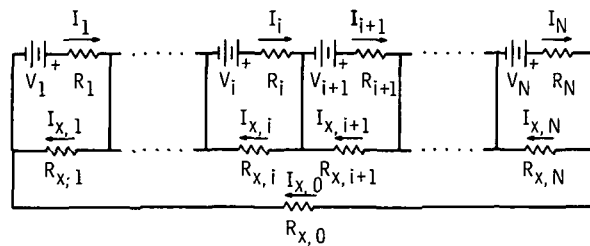


Figure 9. - Equivalent circuit for Hall voltage.

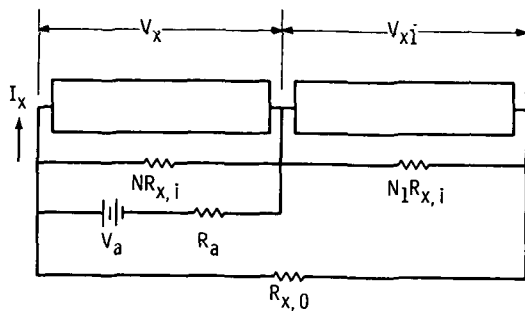


Figure 10. - Equivalent circuit for Hall voltage applied over part of generator.

**Page Intentionally Left Blank**

1. Report No. <b>NASA TM X-2606</b>	2. Government Accession No.	3. Recipient's Catalog No.	
4. Title and Subtitle <b>HALL CURRENT EFFECTS IN THE LEWIS MAGNETOHYDRODYNAMIC GENERATOR</b>		5. Report Date <b>July 1972</b>	6. Performing Organization Code
7. Author(s) <b>Lester D. Nichols and Ronald J. Sovie</b>		8. Performing Organization Report No. <b>E-6924</b>	10. Work Unit No. <b>112-02</b>
9. Performing Organization Name and Address <b>Lewis Research Center National Aeronautics and Space Administration Cleveland, Ohio 44135</b>		11. Contract or Grant No.	13. Type of Report and Period Covered <b>Technical Memorandum</b>
12. Sponsoring Agency Name and Address <b>National Aeronautics and Space Administration Washington, D.C. 20546</b>		14. Sponsoring Agency Code	
15. Supplementary Notes			
16. Abstract <p>Data obtained in the Lewis MHD generator are compared with theoretical values calculated by using the Dzung theory. The generator is operated with cesium seeded argon as the working fluid. The gas temperature varies from 1800 to 2100 K, the gas pressure from 19 to 22 N/cm<sup>2</sup>, the Mach number from 0.3 to 0.5, and the magnetic field strength from 0.2 to 1.6 T. The analysis indicates that there is incomplete seed vaporization and that Hall current shorting paths (through the working fluid to ground at both the entrance and exit of the channel) limit generator performance.</p>			
17. Key Words (Suggested by Author(s)) <b>Magnetohydrodynamic generator Hall current</b>		18. Distribution Statement <b>Unclassified - unlimited</b>	
19. Security Classif. (of this report) <b>Unclassified</b>	20. Security Classif. (of this page) <b>Unclassified</b>	21. No. of Pages <b>26</b>	22. Price* <b>\$3.00</b>

\* For sale by the National Technical Information Service, Springfield, Virginia 22151

NATIONAL AERONAUTICS AND SPACE ADMINISTRATION  
WASHINGTON, D.C. 20546

OFFICIAL BUSINESS  
PENALTY FOR PRIVATE USE \$300

FIRST CLASS MAIL

POSTAGE AND FEES PAID  
NATIONAL AERONAUTICS AND  
SPACE ADMINISTRATION



NASA 451

POSTMASTER: If Undeliverable (Section 158  
Postal Manual) Do Not Return

*"The aeronautical and space activities of the United States shall be conducted so as to contribute . . . to the expansion of human knowledge of phenomena in the atmosphere and space. The Administration shall provide for the widest practicable and appropriate dissemination of information concerning its activities and the results thereof."*

— NATIONAL AERONAUTICS AND SPACE ACT OF 1958

## NASA SCIENTIFIC AND TECHNICAL PUBLICATIONS

**TECHNICAL REPORTS:** Scientific and technical information considered important, complete, and a lasting contribution to existing knowledge.

**TECHNICAL NOTES:** Information less broad in scope but nevertheless of importance as a contribution to existing knowledge.

**TECHNICAL MEMORANDUMS:** Information receiving limited distribution because of preliminary data, security classification, or other reasons.

**CONTRACTOR REPORTS:** Scientific and technical information generated under a NASA contract or grant and considered an important contribution to existing knowledge.

**TECHNICAL TRANSLATIONS:** Information published in a foreign language considered to merit NASA distribution in English.

**SPECIAL PUBLICATIONS:** Information derived from or of value to NASA activities. Publications include conference proceedings, monographs, data compilations, handbooks, sourcebooks, and special bibliographies.

**TECHNOLOGY UTILIZATION PUBLICATIONS:** Information on technology used by NASA that may be of particular interest in commercial and other non-aerospace applications. Publications include Tech Briefs, Technology Utilization Reports and Technology Surveys.

*Details on the availability of these publications may be obtained from:*

**SCIENTIFIC AND TECHNICAL INFORMATION OFFICE**

**NATIONAL AERONAUTICS AND SPACE ADMINISTRATION**

Washington, D.C. 20546